ISSN 1063-7788, Physics of Atomic Nuclei, 2007, Vol. 70, No. 7, pp. 1230–1234. © Pleiades Publishing, Ltd., 2007.
Original Russian Text © T.V. Shchedrina, V. Bradnova, S. Vokál, A. Vokálová, P.I. Zarubin, I.G. Zarubina, A.D. Kovalenko, A.I. Malakhov, G.I. Orlova, P.A. Rukoyatkin, V.V. Rusakova, M. Haidu, S.P. Kharlamov, M.M. Chernyavsky, 2007, published in Yadernaya Fizika, 2007, Vol. 70, No. 7, pp. 1271–1275.

ELEMENTARY PARTICLES AND FIELDS
Experiment

Peripheral Interactions of Relativistic ^{14}N Nuclei with Emulsion Nuclei

T. V. Shchedrina[1)*], V. Bradnova[1)], S. Vokál[2)], A. Vokálová[2)], P. I. Zarubin[1)], I. G. Zarubina[1)], A. D. Kovalenko[1)], A. I. Malakhov[1)], G. I. Orlova[3)], P. A. Rukoyatkin[1)], V. V. Rusakova[1)], M. Haiduc[4)], S. P. Kharlamov[3)], and M. M. Chernyavsky[3)]**

Received April 13, 2006; in final form, November 20, 2006

Abstract—The results of investigation of the dissociation of the 2.86-A-GeV/c ^{14}N nucleus in an emulsion are presented. The cross sections for various fragmentation channels are given. The invariant approach to analysis of fragmentation is used. The momentum and correlation characteristics of the α particles for the $^{14}\mathrm{N} \to 3\alpha + X$ channel in the laboratory system and c.m.s. of three α particles. The results obtained for the ^{14}N nucleus are compared with similar data for the ^{12}C and ^{16}O nuclei.

PACS numbers: 21.45.+v, 23.60+e, 25.10.+s
DOI: 10.1134/S1063778807070149

INTRODUCTION

The fragmentation of relativistic nuclei is a source of information on their structure. The emulsion method makes it possible to thoroughly study the fragmentation of a relativistic projectile nucleus owing to a high resolution of the emulsion and detection of the secondary particles in 4π geometry. The detection of all charged particles and their identification allow investigation of the isotopic composition of the fragments and the fragmentation channels of the projectile nucleus. In this work, nuclear dissociation events conventionally called "white stars" owing to the absence of the traces of the fragments of the target nucleus in them, as well as the decays with the formation of several fragments of the target nucleus, are considered in detail. The main criterion of the selection of these events when studying the projectile-nucleus fragmentation is the requirement of the conservation of the primary charge in a narrow fragmentation cone and the absence of produced charged particles.

EXPERIMENT

A roll consisting of 10×20-cm BR-2 emulsion layers 600 μm in thickness with relativistic sensitivity was irradiated by a 2.86-A-GeV/c ^{14}N nuclear beam from the JINR Nuclotron [1]. The beam was parallel to the emulsion plane along its long side. Events were sought by scanning "along a track" and "over area." The scanning along the track ensures the collection of the data without sampling. This procedure allows us to determine the mean free path of the ^{14}N nucleus in the emulsion. The scanning over the area, which ensures much faster collection of the data, is performed to increase in the sample of events with the most complete destruction of the target nucleus.

The fragment emission angles are measured by a MPE-11 semiautomatic microscope. The microscope is equipped with coordinate maters in the X, Y, and Z axes, whose readings are guided to a PC, where they are processed. The $Z = 1$ fragments of the projectile nucleus are separated from the $Z = 2$ fragments visually, because the ionization of relativistic singly charged particles reliably differs from the four-times larger ionization of doubly charged particles. The fragments with $Z = 3$–7 are separated by the δ-electron count method. The momenta of singly and doubly charged fragments with the emission angles up to 4° are determined from the measurements of multiple Coulomb scattering. The hydrogen and helium isotopes among the fragments of the ^{14}N nucleus are identified from these measurements.

MEAN FREE PATH BEFORE THE INTERACTION

In the total length 123.21 m of the scanned traces, 950 events of the interactions of the ^{14}N nucleus with the nuclei of the elements entering into the emulsion

[1)]Joint Institute for Nuclear Research, Dubna, Moscow oblast, 141980 Russia
[2)]Safarik University, Kosice, Slovak Republic
[3)]Lebedev Physical Institute, Russian Academy of Sciences, Leninskii pr. 53, Moscow, 117924 Russia
[4)]Institute for Space Sciences, Ro-76900, Bucharest-Magurele, Romania
[*]E-mail: shchedrina@lhe.jinr.ru
[**]E-mail: zarubin@lhe.jinr.ru

Table 1. Mean free path λ_{exp} measured for various nuclei in the emulsion and values λ_{theor} calculated by formula [4]

Projectile nucleus	Momentum, A GeV/c	λ_{exp}, cm	λ_{theor}, cm	References
^{4}He	4.5	19.6	19.5 ± 0.3	[1]
^{6}Li	4.5	16.5	14.1 ± 0.4	[1]
^{7}Li	3.0	15.9	14.3 ± 0.4	[2, 3]
^{12}C	4.5	13.5	13.7 ± 0.5	[1]
^{14}N	2.9	13.0	13.0 ± 0.4	This work
^{16}O	4.5	12.1	13.0 ± 0.5	[1]
^{22}Ne	4.1	10.6	10.2 ± 0.1	[1]
^{24}Mg	4.5	10.0	9.6 ± 0.4	[1]

are identified. Thus, the mean free path of the ^{14}N nucleus in the emulsion is equal to $\lambda = 13 \pm 0.4$ cm. This value and λ values for a number of other projectile nuclei in the emulsion that were previously obtained in [2, 3] are presented in Table 1, which also presents the λ_{theor} values calculated by the Bradt–Peters formula [4].

TOPOLOGY OF RELATIVISTIC ^{14}N FRAGMENTATION

Events in which the total charge of the fragments is equal to the projectile-nucleus charge $Z_0 = 7$ and produced particles are absent are selected among 950 found events. The events thus selected are divided into two classes: white-star events (46 events) and events with the formation of one or several target-nucleus fragments (61 events). The white star is a conventional name for events without the target fragments and produced particles. They appear in the case of the minimum energy transfer to the fragmenting nucleus. In this case, the weakest couplings between nucleon clusters in the nucleus are broken and couplings inside the clusters usually remain unchanged. For this reason, they are of particular interest for studying the cluster degrees of freedom in excited nuclei. Another interesting class of events is the simultaneous disintegration of both interacting nuclei with the formation of the fragments of the target nucleus. The fragments of the projectile nucleus in these events are emitted within a narrow forward cone, whose opening angle for fragmenting nucleons is determined by the relation

$$\sin\theta_f = \frac{0.2\ \text{GeV}/c}{p_0},$$

where 0.2 GeV/c is the Fermi momentum and p_0 is the momentum per nucleon of the projectile nucleus. In our case, the fragmentation angle for the primary momentum $p_0 = 2.86$ A GeV/c is equal to 4°.

Table 2. Distribution in the charge topology of white stars and events with the formation of the fragments of the target nucleus in the process of the dissociation of 2.86-A-GeV/c ^{14}N nuclei (Z_{fr} is the heavy-fragment charge, $N_{z=1}$ and $N_{z=2}$ are the number of singly and doubly charged fragments in an event, N_{ws} is the number of white stars, $N_{t.f}$ is the number of stars with the fragments of the target nucleus, and N_Σ is the total number of stars (and their fraction in %)).

Z_{fr}	6	5	5	4	3	3	–	–
$N_{Z=1}$	1	–	2	1	4	2	3	1
$N_{Z=2}$	–	1	–	1	–	1	2	3
N_{ws}	13	4	3	1	1	1	6	17
$N_{t.f.}$	15	1	3	3	–	2	5	32
N_Σ	28	5	6	4	1	3	11	49
N_Σ, %	26	5	5	4	1	3	10	46

For the events satisfying the above conditions, the charge topology of multifragmentation is studied (see Table 2). The first row presents the fragment charge Z_{fr}; the second and third rows present the numbers $N_{Z=1}$ and $N_{Z=2}$ of the singly and doubly charged fragments, respectively; and the fourth and fifth rows are the numbers N_{ws} and $N_{t.f}$ of the events with a given topology for white stars and events with the excitation of the target nucleus for each channel, respectively. The last two rows present the total event number N_Σ and their relative fraction, respectively.

Table 2 shows that the number of the channels containing the fragments with the charges $Z_{fr} > 3$ for both white stars and events with the decay of the projectile nucleus is approximately the same. The channel with the charge configuration $2 + 2 + 2 + 1$ is manifested more clearly in events with the decay of the target than in white stars. Thus, in the events with the decay of the target, the fragmentation of the projectile nucleus is stronger than in white stars. The data presented above indicate the leading role of the

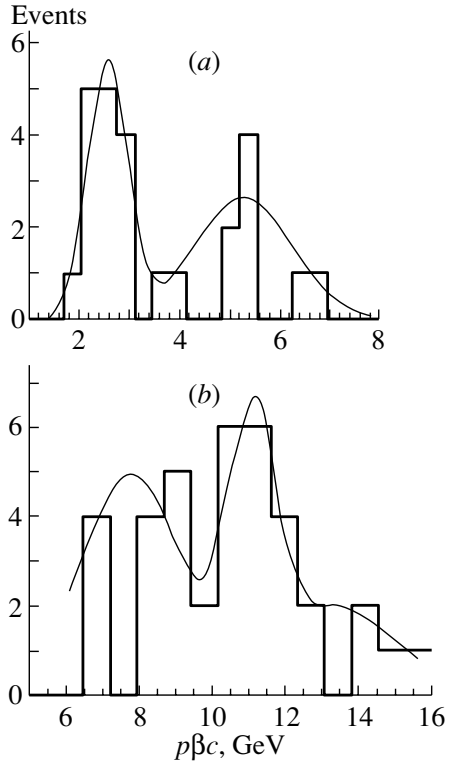

Fig. 1. Histograms of the momentum separation of (a) singly and (b) doubly charged fragments using measurements of $p\beta c$ values for the 2.86-A-GeV/c ^{14}N nucleus. The solid curves are the rms approximations by Gaussians.

channel with the charge configuration $2+2+2+1$ (49 events), which is studied in more detail with a large sample. The mean free path for this channel is equal to $\lambda_{3\mathrm{He}+\mathrm{H}}(^{14}\mathrm{N}) = 2.5 \pm 0.36$ m. The corresponding value for the carbon nucleus is four times larger: $\lambda_{3\mathrm{He}}(^{12}\mathrm{C}) = 10.3 \pm 1.9$ m. The results show that the ^{14}N nucleus is an efficient source for generating 3α systems.

The hydrogen and helium isotopes are separated using the measurements of their $p\beta c$ values under the assumption that the momenta per nucleon of the fragments of the target nucleus is equal to the initial value, i.e., $\mathrm{A_{fr}} = (p\beta c)/(p_0\beta c)$. The multiple Coulomb scattering method used to determine the momenta is based on the following relation between the mean particle deviation $\langle|D|\rangle$ in cells with the length t and the quantity $p\beta c$:

$$\langle|D|\rangle = \frac{Z_{\mathrm{fr}} K t^{3/2}}{573 p\beta c},$$

where Z_{fr}, p, and βc are the charge, momentum, and velocity of the particle, respectively, and K is the known scattering constant. For multiple Coulomb scattering, the distribution in $p\beta c$ for individual particles with the same charge and momentum must be close to a normal distribution. For this reason, the distribution in $p\beta c$ for a group of the fragments with the same velocity and charge but with different masses must be a superposition of several normal distributions.

Figure 1 shows the results of measurements of the multiple scattering of singly and doubly charged fragments. The momenta measured for the singly charged fragments are satisfactorily described by the sum of two Gaussians whose maxima are at 2.6 and 5.6 GeV and correspond to the ^{1}H and ^{2}H isotopes (Fig. 1a). The ^{1}H-to-^{2}H yield ratio is approximately equal to 2 : 1. This indicates that the deuteron fraction in our case is noticeably lower than that for the relativistic fragmentation of the ^{6}Li ($2+1$ channel) and ^{10}B ($2+2+1$ channel) nuclei, where the yields of the protons and deuterons are approximately equal to each other.

Figure 1b shows the distribution of 37 doubly charged fragments in measured $p\beta c$ values. This distribution is satisfactorily approximated by the sum of two normal distributions (the solid curve in the figure). The maxima of the approximating distribution are located at $p\beta c = 7.8$ and 11.3 GeV, which are sufficiently close to the $p\beta c$ values corresponding to the ^{3}He and ^{4}He isotopes. The percent yields of the ^{3}He and ^{4}He fragments are equal to about 40 and 60%, respectively. Several helium isotopes observed for $p\beta c$ values from 14 to 16 GeV are identified as ^{6}He (5% of the total number of events). We are going to perform more detailed analysis for events with the formation of the ^{6}He isotope.

MOMENTUM AND CORRELATION CHARACTERISTICS OF Nα SYSTEMS

After the increase in the collected statistics by means of the scanning over the area of the emulsion layers, the number of $^{14}\mathrm{N} \to 3\alpha + X$ events is equal to 132, including 50 white stars. Let us consider the basic kinematic characteristics of relativistic α particles, which are the fragments of the projectile nucleus from the $^{14}\mathrm{N} \to 3\alpha + X$ reaction, and compare them with the characteristics from the $^{12}\mathrm{C} \to 3\alpha$ and $^{16}\mathrm{O} \to 4\alpha$ reactions. Figure 2a shows the distribution in the transverse-momentum squared of α particles in the laboratory system for the $^{14}\mathrm{N} \to 3\alpha + X$ channel. The transverse momenta p_t are calculated by the formula

$$p_t = 4p_0 \sin\theta;$$

i.e., analysis of p_t distributions means analysis of the angular distributions of α particles. This distribution has a break near $p_t^2 = 0.05\,(\mathrm{GeV}/c)^2$. The solid curve corresponds to the sum of two Rayleigh distributions.

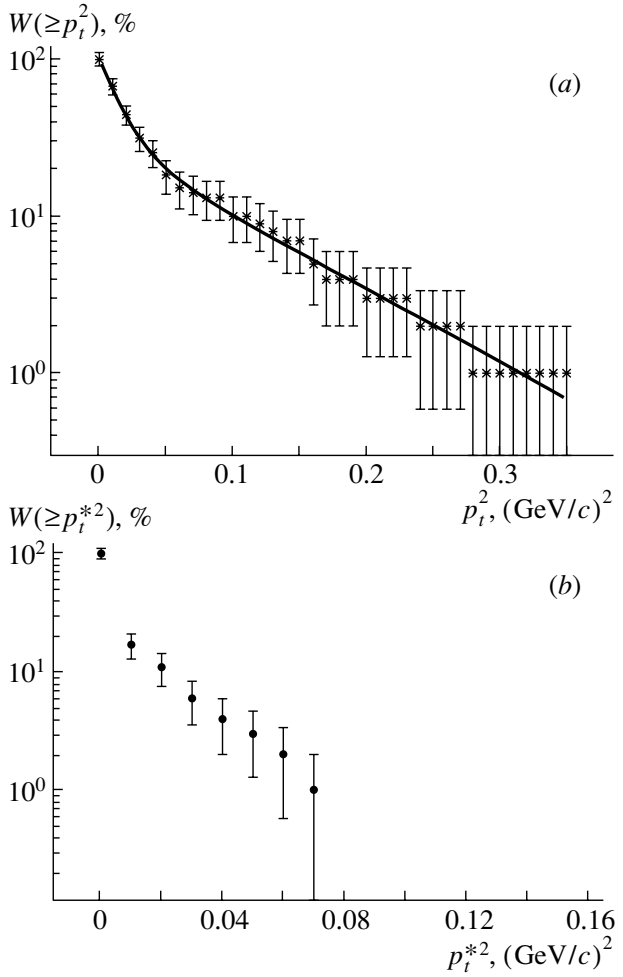

Fig. 2. Distributions of the α particles from the $^{14}\mathrm{N} \to 3\alpha + X$ reactions in p_t^2 (a) in the laboratory system and (b) in the rest frame of 3α particles. The solid curve is the sum of two Rayleigh distributions.

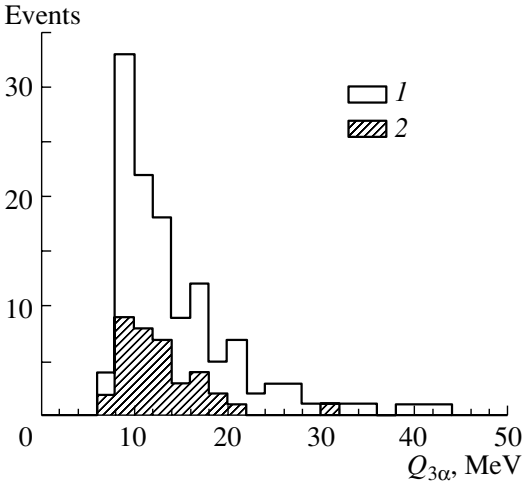

Fig. 3. Distribution in the invariant excitation energy $Q_{3\alpha}$ of the 3α system with respect to the ground state of the ^{12}C nucleus in the $^{14}\mathrm{N} \to 3\alpha + \mathrm{X}$ process for (*1* all the events of this dissociation reaction and *2* white stars).

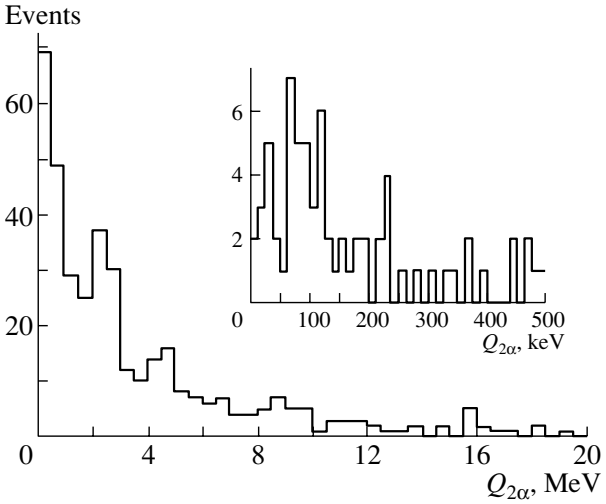

Fig. 4. Distribution in the invariant excitation energy $Q_{2\alpha}$ of pairs of α particles for the $^{14}\mathrm{N} \to 3\alpha + \mathrm{X}$ process. The inset shows the distribution in the range 0–500 keV.

The momenta in the 3α system can be calculated by subtracting the momentum acquired by the system in interaction:

$$\mathbf{p}_t^* = \mathbf{p}_t - \sum \mathbf{p}_{ti}/3.$$

The distribution in p_t^* for α particles in the $^{14}\mathrm{N} \to 3\alpha + X$ reaction is shown in Fig. 2*b*. In agreement with expectation, the mean values of p_t^* are much lower than those in the laboratory system and are the same within the error for the ^{14}N, ^{12}C [5], and ^{16}O nuclei [6].

To estimate the energy scale of the formation of 3α systems in the $^{14}\mathrm{N} \to 3\alpha + X$ channel, we consider the distribution in the invariant excitation energy Q with respect to the ground state of the ^{12}C nucleus:

$$Q = M^* - M.$$

Here, M is the mass of a nucleus corresponding to the charge and weight of the system and M^* is the invariant mass of the system of the fragments:

$$M^{*2} = (\Sigma P_j)^2 = \Sigma(P_i P_k),$$

where $P_{i,k}$ is the 4-momenta of the ith and kth fragments.

Most events are concentrated in the $Q_{3\alpha}$ range from 10 to 14 MeV, which includes known ^{12}C levels (Fig. 3). The softening of the selection conditions for $3\mathrm{He} + \mathrm{H}$ events, which allows the formation of the fragments of the target, does not lead to the shift of the peak of 3α excitations. This circumstance indicates

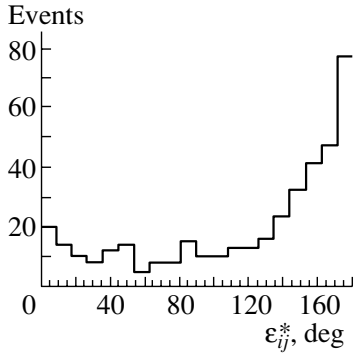

Fig. 5. Distribution in the pair azimuth angle ε^*_{ij} in the rest frame of 3α particles for the $^{14}\mathrm{N} \to 3\alpha + \mathrm{X}$ process.

that the mechanism of the occupation of 3α states is universal.

To estimate the fraction of events with the formation of the ^{8}Be intermediate nucleus in the $^{14}\mathrm{N} \to {}^8\mathrm{Be} + \alpha + X \to 3\alpha + X$ reactions, we consider the distribution in the invariant excitation energy of a pair of α particles with respect to the ground state of the ^{8}Be nucleus (Fig. 4). The first peak of the distribution corresponds to the value expected for the products of the decay of the unstable ^{8}Be nucleus in the 0^+ ground state. This part of the spectrum is shown in the inset in Fig. 4 in the 20 : 1 scale. As seen, the center of the distribution coincides with the decay energy of the ^{8}Be ground state. According to the existing statistics, the fraction of pairs of α particles from the decay of the ^{8}Be nucleus is equal to 25–30%.

The role of the ^{8}Be nucleus is clearly manifested in a strongly asymmetric distribution in the pair azimuth angle ε^*_{ij} of pairs of α particles in the rest frame of 3α particles from the $^{14}\mathrm{N} \to 3\alpha + X$ reaction (Fig. 5). The asymmetry of the distribution in the pair azimuth angle ε^*_{ij} is also observed for α fragments in the c.m.s. for the decay of the nuclei ^{12}C [5] and ^{16}O [6]. The azimuthal asymmetry coefficients and collinearity coefficients for ^{14}N coincide within the errors with the respective coefficients for ^{12}C and significantly differ from the respective coefficients for $^{16}\mathrm{O} \to 4\alpha$. This difference can be explained both by more complex combination of α particles for the last nucleus and by the possibility for α fragments to be the products of the decay of other intermediate unstable states.

CONCLUSIONS

The distribution in charge topology in the dissociation of 2.86-A-GeV/c ^{14}N nuclei interacting with the emulsion nuclei indicates the leading role of the channel with the $2 + 2 + 2 + 1$ charge configuration.

Preliminary analysis shows that the proton-to-deuteron ratio for the $^{14}\mathrm{N} \to 3\alpha + \mathrm{H}$ channel is $N_p : N_d \approx 2$ and the helium isotope ratio is $^4\mathrm{He} : {}^3\mathrm{He} \approx 1.5$. Several events (5% of the total number of events) of the formation of the ^{6}He isotope are identified, which requires more detailed additional analysis.

The distributions in the pair azimuth angle ε^*_{ij} between the He fragments of the ^{14}N nuclei in the c.m.s. are asymmetric with the excess in the range 140°–180°, as for the ^{12}C and ^{16}O nuclei.

The estimate of the energy scale of the formation of 3α systems shows that 80% of currently identified events are concentrated in the range 10–14 MeV. The fraction of the $^{14}\mathrm{N} \to {}^8\mathrm{Be} + \alpha + X \to 3\alpha + X$ channel with the formation of the ^{8}Be intermediate nucleus is $\approx 25\%$.

ACKNOWLEDGMENTS

This work was supported by the Russian Foundation for Basic Research (project nos. 96-1596423, 02-02-164-12a, 03-02-16134, 03-02-17079, and 04-02-16593), by the Agency of Science, Ministry of Education of the Slovak Republic and Slovak Academy of Sciences (grant no. VEGA 1/2007/05), and by the Plenipotentiaries of Bulgaria, Slovak Republic, Czech Republic, and Romania at JINR (projects in 2002–2005).

REFERENCES

1. The BECQUEREL Project, http://becquerel.jinr.ru.
2. M. I. Adamovich et al., Yad. Fiz. **62**, 1461 (1999) [Phys. At. Nucl. **62**, 1378 (1999)].
3. M. I. Adamovich et al., J. Phys. G **30**, 1479(2004).
4. H. Bradt and B. Peters, Phys. Rev. **77**, 54(1950).
5. V. V. Belaga et al., Yad. Fiz. **58**, 2014 (1995) [Phys. At. Nucl. **58**, 1905 (1995)].
6. F. A. Avetyan et al., Yad. Fiz. **59**, 110 (1996) [Phys. At. Nucl. **59**, 102 (1996)].

Translated by R. Tyapaev